



HHS Public Access

Author manuscript

Nat Chem. Author manuscript; available in PMC 2012 June 01.

Published in final edited form as:

Nat Chem. ; 3(12): 943–948. doi:10.1038/nchem.1198.

Dynamic Multi-Component Covalent Assembly for the Reversible Binding of Secondary Alcohols and Chirality Sensing

Lei You, Jeffrey S. Berman, and Eric V. Anslyn*

Department of Chemistry and Biochemistry, The University of Texas at Austin, Austin, TX 78712 USA

Abstract

Reversible covalent bonding is often employed for the creation of novel supramolecular structures, multi-component assemblies, and sensing ensembles. In spite of remarkable success of dynamic covalent systems, the reversible binding of a mono-alcohol with high strength is challenging. Here we show that a strategy of carbonyl activation and hemiaminal ether stabilization can be embodied in a four-component reversible assembly that creates a tetradentate ligand and incorporates secondary alcohols with exceptionally high affinity. Evidence is presented that the intermediate leading to binding and exchange of alcohols is an iminium ion. Further, to demonstrate the use of this assembly process we explored chirality sensing and enantiomeric excess determinations. An induced twist in the ligand by a chiral mono-ol results in large Cotton effects in the circular dichroism spectra indicative of the alcohol's handedness. The strategy revealed in this study should prove broadly applicable for the incorporation of alcohols into supramolecular architecture construction.

The study of dynamic multi-component assemblies created from reversible covalent bonds is at the forefront of recent supramolecular chemistry efforts, with the ultimate goals of creating molecular machines, complex nanoarchitectures, dynamic combinatorial libraries, and sensors^{1,2,3,4,5,6,7}. Although the addition of amines to carbonyls to create imines^{8,9,10,11} or hemiaminals^{12,13}, and the association of boronic acids with diols to form cyclic boronate esters^{14,15}, have been widely explored as reversible systems, the use of simple mono-alcohols is exceedingly rare due to their poor nucleophilicity^{16,17}. This is despite the fact that alcohols, especially secondary alcohols, are common functional groups found in natural products, such as terpenes, saccharides, and polyketides, as well as polymeric materials, such as polyvinyl alcohol. In addition, chiral alcohols are frequently sought after in asymmetric reactions, such as allylation of aldehydes and hydrogenation of

Users may view, print, copy, download and text and data-mine the content in such documents, for the purposes of academic research, subject always to the full Conditions of use: http://www.nature.com/authors/editorial_policies/license.html#terms

Correspondence and requests for materials should be addressed to E.V.A., anslyn@austin.utexas.edu.

Author contributions

L.Y. and E.V.A. developed the strategy and the mechanistic concepts. L.Y. performed the experiments. J.S.B. participated in the reaction optimization. E.V.A. directed the research. L.Y. and E.V.A. wrote the manuscript.

Author information

Reprints and permissions information is available at www.nature.com/reprints. The authors declare no competing financial interests. Supplementary Information and chemical compound information accompany this paper at www.nature.com/naturechemistry. Reprints and permissions information is available online at <http://npg.nature.com/reprintsandpermissions/>.

ketones^{18, 19, 20, 21}, to name just a few synthetic transformations. Hence, the diversity of supramolecular architectures that could be created would be greatly expanded with a strategy for the reversible binding of mono-ols, and the new strategy could have the potential for molecular sensing applications.

Compared to an amine used for imine formation^{22,23,24}, a mono-ol is far less nucleophilic. Therefore, their carbonyl addition products, hemiacetals and acetals, are more sluggish to form than imines without Brønsted catalysis, and they are less thermodynamically favorable^{25,26,27,28}. The sluggishness is exacerbated with secondary and tertiary alcohols whose addition products are more sterically congested than those from primary alcohols. Hence, approaches to the reversible binding of secondary and tertiary alcohols are nearly nonexistent in the literature, either by covalent or noncovalent strategies. In order to achieve the binding of mono-ols in a reversible covalent manner, electron-withdrawing groups, commonly trifluoromethyl, are placed on carbonyls^{29,30,31}. Our group and Lehn recently reported that 2-acylpyridines (**1**) reversibly add secondary alcohols when activated by a Brønsted acid, or a Lewis acid such as Zn(OTf)₂ (e.g. Fig. 1a)^{16,17}. Unfortunately, such systems are moisture sensitive, and subsequently we have found are not readily adaptable to increased complexity, nor to any chirality sensing applications, as is the goal of much of our group's efforts³².

Iminium functional groups represent an excellent alternative to carbonyls because of their increased electrophilicity. Iminium salts are routinely intermediates in reaction sequences, and they are commonly generated *in situ*^{33,34,35}. We therefore postulated that they would rapidly add alcohols to create hemiaminal ethers^{36,37}, but also readily expel the alcohol recreating the iminiums³⁸. Hence, iminium ions were thought to possess the desired reversibility, but a lack of thermodynamic stability of the resulting hemiaminal ethers. Therefore, we sought a system where iminiums could be formed, reversibly add secondary alcohols, yet with the resulting hemiaminal ethers thermodynamically stabilized via a remote binding process. To the best of our knowledge, the system reported here represents the first example of iminiums for dynamic mono-ol binding and chirality sensing, even though there is a rich history of using iminiums in synthetic organic chemistry^{32,33,34,35,37}.

Results and discussion

To realize our new strategy with a specific chemical design, we built upon a three-component assembly reaction which spontaneously occurs upon mixing the reactants shown in Fig. 1b³⁹. We reasoned that if the product of this reaction (**2**) could be induced to eliminate water, iminium ion **3** would form. Once formed, this reactive intermediate would add alcohols, and the resulting tris(pyridine) ligand would chelate the Zn(II) to stabilize addition product **4** (Fig. 1c). In essence, the reactivity of the iminium and the thermodynamic stability of the metal complex were postulated to provide the driving force for the otherwise unfavorable binding of a secondary alcohol.

With our concept in mind, we first set out to explore the four-component assembly given in Fig. 1d with isopropyl alcohol (**IPA**) as the test alcohol. Pyridine-2-carboxaldehyde (**2-PA**), di-(2-pyridylmethyl)amine (**DPA**), Zn(OTf)₂ and **IPA** were stirred in acetonitrile with

activated 3 Å molecular sieves (MS). The dominant product was **2**, and only a trace of reaction with **IPA** was observed within 24 hours (Supplementary Fig. S1). It is known that Brønsted acids facilitate imine and iminium formation from hemiaminals⁴⁰, and therefore a series of acids were screened: triethylammonium chloride, pyridinium triflate, imidazolium triflate, and 4-(2-chloroethyl)morpholine hydrochloride (CEM-HCl). The four-component reactions were stirred with 3 Å MS at 24 °C with one equivalent of each of these acids (molar ratio of **2-PA**, Zn(OTf)₂, **DPA**, and **IPA**: 1: 1: 1.2: 5; with 30–40 mM of **2-PA**), and the equilibrium was reached after 20 h, all resulting in formation of **4**, but to differing extents (Supplementary Fig. S2). CEM-HCl was the most effective, yielding ~90% of **4** with residual **2** and **2-PA** remaining.

In addition to the effect of p*K*_a of the Brønsted acid catalyst on the reaction, there was a difference between chloride and triflate salts on the extent of the assembly, and hence, a counterion effect study on the multi-component reaction was performed. Pyridinium triflate was chosen as the catalyst, and various anions, including Cl⁻, Br⁻, I⁻, acetate (AcO⁻), and benzoate (BzO⁻), were investigated. The four-component assembly reaction was performed in the presence of pyridinium triflate and tetrabutylammonium salts of different anions. Cl⁻, Br⁻, and I⁻ were found to increase the formation of complex **4** to approximately 88%, 84%, and 81%, respectively (~65% of **4** formed with only pyridinium triflate. Supplementary Fig. S3). This effect is likely due to stabilization of the complex by halogen coordination in the axial position of the zinc center, and the effect accounts for the difference between chloride and triflate salts because of the non-coordinating property of triflate. However, for AcO⁻ and BzO⁻ the effect is smaller. The p*K*_a of AcOH and BzOH in acetonitrile is 23.5 and 21.5 respectively⁴¹, while the p*K*_a of pyridinium in acetonitrile is 12.5⁴². It is therefore obvious that the real acid catalyst is AcOH and BzOH due to the acid-base reaction between pyridinium and AcO⁻ or BzO⁻, respectively.

To demonstrate the generality and reversibility of the four-component assembly, alcohol component exchange was studied. If the assembly was initially formed with **IPA**, after addition of 3-methyl-2-butanol complex **4** decreased over a period of 20 hours with a concomitant increase of the analogous assembly product incorporating 3-methyl-2-butanol (two sets of ¹H NMR resonances due to diastereomer formation, Fig. 2a). The equilibrium constant for the reaction of **4** (created from **IPA**) with 3-methyl-2-butanol is 0.74, therefore slightly preferring **4** likely due to less steric interactions. Analogous spectra show the equilibrium constant (*K*_{eq}) for the reaction of **4** with 3,3-dimethyl-2-butanol to be 0.48. The *K*_{eq} values with other alcohols are listed in Fig. 2b, and are consistent with the bulkiness of the alcohol. It is worthwhile to note that the four-component assembly with each secondary alcohol studied was successful and led to their respective complex (such as **4** with **IPA**).

We then set out to explore aldehyde component exchange as a means to increase the diversity and complexity of the assembly, and further verify reversibility. **2-PA**, isoquinoline-2-carboxyaldehyde, 5-bromo-pyridine-2-carboxyaldehyde, thiazole-2-carboxyaldehyde, and thiazole-4-carboxyaldehyde were all studied. For example, the assembly was performed with thiazole-2-carboxyaldehyde followed by addition of **2-PA**, and the mixture was stirred for 20 h. ¹H NMR indicated the increase of the **2-PA** derived complex with a concomitant decrease of assembly incorporating thiazole-2-carboxyaldehyde (Fig. 2c).

The K_{eq} values are summarized in Fig. 2d, which shows that **2-PA** is the aldehyde giving the most complex in the cases studied. Both the electrophilicity of the aldehyde and the Lewis basicity of the pyridine ligand clearly have an effect on aldehyde exchange.

The next goal was to determine the equilibrium constant of the four-component assembly using **IPA** as a model alcohol. Because of the difficulty of quantifying the effect of molecular sieves (MS), the assembly was conducted without MS, and as expected, the extent of **4** decreased while **2** increased (Supplementary Fig. S12). An equal equivalent of **4** and water is generated by the reaction. Because the Brønsted acid is not incorporated into **2** or **4**, it was not taken into consideration for the calculation of K_{eq} . Moreover, **DPA** and tris(pyridine)amine ligands (**2** and **4**, respectively) have much higher affinities for zinc than **2-PA**, and hence, the non-reactive zinc was assumed to be bound to the remaining **DPA** to create **Zn-DPA**. As a result, the three and four-component assemblies shown in Figure 1b and 1d were simplified to two and three-component systems (Eqs. 1 and 2), respectively. Substituting Eq. 1 into Eq. 2 affords Eq. 3. The stability constant of **Zn-DPA** is given by Eq. 4, which when combining with Eq. 3 gives the K_{eq} expression for the four-component assembly (Eqs. 5 and 6, see details in Supplementary Information).

$$K(\mathbf{2}) = \frac{[\mathbf{2}]}{[\mathbf{2} - \text{PA}] [\text{Zn} - \text{DPA}]} \quad (1)$$

$$K(\mathbf{4}) = \frac{[\mathbf{4}] [\text{H}_2\text{O}]}{[\mathbf{2} - \text{PA}] [\text{Zn} - \text{DPA}] [\text{IPA}]} \quad (2)$$

$$K(\mathbf{4}) = \frac{K(\mathbf{2}) [\mathbf{4}]^2}{[\mathbf{2}] [\text{IPA}]} \quad (3)$$

$$K(\text{Zn} - \text{DPA}) = \frac{[\text{Zn} - \text{DPA}]}{[\text{Zn}] [\text{DPA}]} \quad (4)$$

$$K_{\text{eq}} = K(\mathbf{4}) K(\text{Zn} - \text{DPA}) \quad (5)$$

$$K_{\text{eq}} = \frac{K(\mathbf{2}) K(\text{Zn} - \text{DPA}) [\mathbf{4}]^2}{[\mathbf{2}] [\text{IPA}]} \quad (6)$$

All concentrations in Eq. 6 can be deduced from ^1H NMR integrals and the mass balance of **2-PA** as well as **IPA**. Using the reported value for $K(\mathbf{2})$ ³⁹ and $K(\text{Zn-DPA})$ ^{43,44}, the K_{eq} of the multi-component assembly incorporating **IPA** (Fig. 1d) was estimated to be on the order of 10^8 – 10^9 M^{-2} . Such a high equilibrium constant demonstrates the power of our multi-component approach and is unprecedented for the reversible binding of mono-ols. The equilibrium constant with other alcohols or aldehydes can be calculated as a product of K_{eq} for **IPA** with the corresponding K_{eq} of the related component exchange reaction.

The scrambling of alcohols and aldehydes in structures such as **4** logically proceeds via iminium **3** or its analogs derived from aldehydes other than **2-PA** (Fig. 3a, **3** as an illustrative example). During the four-component assembly (Fig. 1d), we observe via ^1H NMR spectroscopy that complex **2** is formed first and evolves over time to structure **4** because the 3\AA MS scavenges water, thereby driving the equilibrium to alcohol incorporation. Therefore, the proposed sequence involves compound **2** formed from **2-PA**, **DPA**, and $\text{Zn}(\text{OTf})_2$, dissociating from $\text{Zn}(\text{II})$, followed by water elimination catalyzed by the Brønsted acid to give iminium **3**, which in turn adds alcohol and re-coordinates $\text{Zn}(\text{II})$ to give **4**, all species in equilibrium. Obviously, this sequence of steps involving **3** as an intermediate would scramble alcohols (R^1OH for R^2OH in Fig. 3a). To scramble aldehydes via iminium **3**, water would add followed by **DPA** elimination, with or without **2** as an intermediate.

The following observations further support that the intermediate of the assembly is iminium **3**. First, an equilibrium mixture of **2-PA**, **DPA**, $\text{Zn}(\text{OTf})_2$ with **2** (3\AA MS added) afforded the same results as the four-component assembly after addition of **IPA** and CEM-HCl (Fig. 3b). In contrast, **2-PA** and **IPA** in the presence of $\text{Zn}(\text{OTf})_2$ and 3\AA MS did not give significant extents of hemiacetal products via ^1H NMR, but subsequent addition of **DPA** and CEM-HCl to this mixture gave a similar equilibrium mixture containing **4** (Supplementary Fig. S14). Further, ESI mass spectral analysis supports the postulate that **3** is a viable structure (Fig. 3c). A peak corresponding to this compound was found, while mass analysis again found no evidence of hemiacetals or acetals derived from **2-PA**. Therefore, we postulate that the four-component assembly does not commence via hemiacetal formation from **2-PA** and **IPA**. Instead, we propose that iminium **3** is the key intermediate that leads to scrambling between water and alcohols and between alcohols or aldehydes.

To exploit the multi-component assembly for chirality sensing purposes, the binding of enantiomerically pure chiral secondary alcohols was explored. The analysis of chirality by optical methods is currently of interest for high-throughput screening of enantiomeric excess (*ee*) values of catalytic asymmetric reactions^{15,32,45}. The faces of iminium ion **3** are enantiotopic, and therefore the addition of **IPA** simply creates enantiomers. The methyls of the isopropyl group become diastereotopic, which is observed in the ^1H NMR spectra (see Supplementary Information). However, when chiral alcohols are used diastereomers of **4** are created. The resulting diastereomeric ratios (*dr*, defined as the concentration ratio of the major diastereomer over the minor diastereomer) were measured by ^1H NMR *via* integrating the methine hydrogens on the newly formed stereocenter, as well as the hydrogens of the chiral alcohol. Pure enantiomers of each alcohol show the same *dr*, albeit involving an enantiomeric set of diastereomers (Supplementary Fig. S16 and S18). For 1-phenylethanol, the *dr* values are above 2, while for 2-butanol the ratios are more modest (1.3, *see* Fig. 4a). 3-Methyl-2-butanol has a *dr* value of 1.7. The trend of *dr* values is consistent with the relative size of the two R-groups on the alcohol's stereocenters, which dictate the preferred handedness on the newly formed stereocenter. The fact that significant *dr* values exist paved the way for an optical spectroscopy method of determining alcohol handedness and corresponding *ee* values.

The assembled Zn(II) ligands will have a preferential M (clockwise) or P (counterclockwise) twist that depends upon the handedness of the stereocenter formed in the tris(pyridine) ligand^{46,47}. The twist can be observed as a Cotton effect⁴⁸ in CD spectra resulting from exciton coupled circular dichroism (ECCD)¹⁰. ECCD has been successfully used to signal the handedness of chiral aminoalcohols⁴⁹, vicinal diols⁵⁰, and epoxyalcohols⁵¹, while the one case it was used for mono-ol sensing gave very weak signals and the binding mode was unclear⁵². There are no CD spectra of the starting components listed in Fig. 1d, as well as the chiral alcohols, above 225 nm. However, the four-component assembly led to large and reproducible signals. CD spectra of diluted solutions (from the experimental conditions described above) of the assemblies for six chiral alcohols are shown in Fig. 4b. *S*-stereocenters in the alcohols resulted in positive Cotton effects at 269 nm while the *R*-stereocenters gave equal intensity negative Cotton effects. Hence, the sign of the Cotton effect is indicative of the handedness of the alcohol stereocenter. The signal intensity follows the order: 1-phenylethanol > 3-methyl-2-butanol > 2-butanol, which is in accordance with the order of *dr* values.

We next set out to quantify *ee* values by CD measurements using 1-phenylethanol as a model alcohol. The assembly reactions were conducted using three equivalents of alcohol to ensure the signal was saturated. To ensure reproducibility, *ee* calibration curves were constructed using data at 11 *ee* values (−100, −80, −60, −40, −20, 0, 20, 40, 60, 80, 100 %) with each point being repeated by three independent assembly reactions and measurements. The CD spectra for assembly from 1-phenylethanol with various *ee* were shown in Fig. 4c and the reproducibility of the data at 251 and 269 nm was excellent (Fig. 4d). Both peaks gave linear calibration lines with R^2 around 0.99 (Supplementary Fig. S26). The CD spectra of twelve test samples of varying *ee* values were recorded, and the calibration curve at 269 nm was used to calculate the *ee*. The average absolute error was 2.3% for 1-phenylethanol (Supplementary Table S1). Such high accuracy for an optical method is rare, and is more than sufficient for the screening of asymmetric reactions³². In addition, we expect no hurdle to expand the specific *ee* assay to other chiral secondary alcohols.

In summary, the multi-component assembly reaction described herein leads to the thermodynamic stabilization of hemiaminal ethers derived from secondary alcohols and an activated iminium ion via the use of remote metal coordination. The reversibility and dynamics of the system are demonstrated by counterion effects, as well as alcohol and aldehyde component exchange. Because the multi-component assembly incorporates simple mono-ols, and because only readily available commercial reagents are used, the general strategy has broad utility for the binding of alcohols in many scenarios. As one example, we exploited the strategy in conjugation with CD analysis to successfully classify secondary alcohol chirality via the sign of Cotton effects, as well as quantitate *ee* values in a simple fashion with surprisingly high accuracy for an optical method. Current efforts are focused on using the general assembly strategy for dynamic library creation, as well as recognition and discrimination of chiral alcohols.

METHODS

General procedure: to a stirred solution of **2-PA** (30–40 mM, 1 equiv.) and $\text{Zn}(\text{OTf})_2$ (1 equiv.) in acetonitrile, were added activated 3Å molecular sieves (4 to 8 mesh), **DPA** (1.2 equiv.), a mono-ol (2–5 equiv.), and CEM-HCl (1 equiv.). The mixture was stirred at room temperature overnight. The assembly solution was characterized by ^1H NMR, ESI mass spectrometry or CD. For full experimental details and spectra data, dynamics studies as well as chirality analysis, see Supplementary Information.

Supplementary Material

Refer to Web version on PubMed Central for supplementary material.

Acknowledgments

We thank Ben Shoulders and Steve Sorey for NMR assistance, Karin Keller for mass spectrometric assistance, and Eun Jeong Cho of the Texas Institute for Drug and Diagnostic Development. We are grateful to financial support provided by the National Institute of Health (GM 077437) and the Welch Foundation (F-1151).

References

1. Rowan SJ, et al. Dynamic covalent chemistry. *Angew Chem Int Ed.* 2002; 41:898–952.
2. Corbett PT, et al. Dynamic combinatorial chemistry. *Chem Rev.* 2006; 106:3652–3711. [PubMed: 16967917]
3. Lehn JM. From supramolecular chemistry towards constitutional dynamic chemistry and adaptive chemistry. *Chem Soc Rev.* 2007; 36:151–160. [PubMed: 17264919]
4. Hunt RAR, Otto S. Dynamic combinatorial libraries: new opportunities in systems chemistry. *Chem Commun.* 2011; 47:847–858.
5. Mastalerz M. Shape-persistent organic cage compounds by dynamic covalent bond formation. *Angew Chem Int Ed.* 2010; 49:5042–5053.
6. Mohr GJ. Chromo- and fluororeactands: indicators for detection of neutral analytes by using reversible covalent-bond chemistry. *Chem Eur J.* 2004; 10:1082–1090. [PubMed: 15007799]
7. Christinat N, Scopelliti R, Severin K. Multicomponent assembly of boronic acid based macrocycles and cages. *Angew Chem Int Ed.* 2008; 47:1848–1852.
8. Meyer CD, Joiner CS, Stoddart JF. Template-directed synthesis employing reversible imine bond formation. *Chem Soc Rev.* 2007; 36:1705–1723. [PubMed: 18213980]
9. Beeren SR, Sanders JK. Discovery of linear receptors for multiple dihydrogen phosphate ions using dynamic combinatorial chemistry. *J Am Chem Soc.* 2011; 133:3804–3807. [PubMed: 21361379]
10. Osowska K, Miljanic OS. Oxidative kinetic self-sorting of a dynamic imine library. *J Am Chem Soc.* 2011; 133:724–727. [PubMed: 21171598]
11. Park H, et al. Bioinspired chemical inversion of L-amino acids to D-amino acids. *J Am Chem Soc.* 2007; 129:1518–1519. [PubMed: 17283992]
12. Reinert S, Mohr GJ. Chemosensor for the optical detection of aliphatic amines and diamines. *Chem Commun.* 2008:2272–2274.
13. Mertz E, Beil JB, Zimmerman SC. Kinetics and thermodynamics of amine and diamine signaling by a trifluoroacetyl azobenzene reporter group. *Org Lett.* 2003; 5:3127–3130. [PubMed: 12916998]
14. Zhao J, Fyles TM, James TD. Chiral binol-bisboronic acid as fluorescent sensor for sugar acids. *Angew Chem Int Ed.* 2004; 43:3461–3464.
15. Shabbir SH, Regan CJ, Anslyn EV. A general protocol for creating high-throughput screening assays for reaction yield and enantiomeric excess applied to hydrobenzoin. *Proc Natl Acad Sci U S A.* 2009; 106:10487–10492. [PubMed: 19332790]

16. You L, Anslyn EV. Secondary alcohol hemiacetal formation: an in situ carbonyl activation strategy. *Org Lett.* 2009; 11:5126–5129. [PubMed: 19835394]
17. Drahonovsky D, Lehn JM. Hemiacetals in dynamic covalent chemistry: formation, exchange, selection, and modulation processes. *J Org Chem.* 2009; 74:8428–8432. [PubMed: 19799441]
18. Denmark SE, Fu J. Catalytic enantioselective addition of allylic organometallic reagents to aldehydes and ketones. *Chem Rev.* 2003; 103:2763–2794. [PubMed: 12914480]
19. Walsh PJ. Titanium-catalyzed enantioselective additions of alkyl groups to aldehydes: mechanistic studies and new concepts in asymmetric catalysis. *Acc Chem Res.* 2003; 36:739–749. [PubMed: 14567707]
20. Ikariya T, Blacker AJ. Asymmetric transfer hydrogenation of ketones with bifunctional transition metal-based molecular catalysts. *Acc Chem Res.* 2007; 40:1300–1308. [PubMed: 17960897]
21. Skucas E, Ngai MY, Komanduri V, Krische MJ. Enantiomerically enriched allylic alcohols and allylic amines via C-C bond-forming hydrogenation: asymmetric carbonyl and imine vinylation. *Acc Chem Res.* 2007; 40:1394–1401. [PubMed: 17784728]
22. Xu S, Giuseppone N. Self-duplicating amplification in a dynamic combinatorial library. *J Am Chem Soc.* 2008; 130:1826–1827. [PubMed: 18211071]
23. Folmer-Andersen JF, Lehn JM. Constitutional adaptation of dynamic polymers: hydrophobically driven sequence selection in dynamic covalent polyacylhydrazones. *Angew Chem Int Ed.* 2009; 48:7664–7667.
24. Dirksen A, Dirksen S, Hackeng TM, Dawson PE. Nucleophilic catalysis of hydrazone formation and transimination: implications for dynamic covalent chemistry. *J Am Chem Soc.* 2006; 128:15602–15603. [PubMed: 17147365]
25. Funderburk LH, Aldwin L, Jencks WP. Mechanisms of general acid and base catalysis of the reactions of water and alcohols with formaldehyde. *J Am Chem Soc.* 1978; 100:5444–5459.
26. Fuchs B, Nelson A, Star A, Stoddart JF, Vidal S. Amplification of dynamic chiral crown ether complexes during cyclic acetal formation. *Angew Chem Int Ed.* 2003; 42:4220–4224.
27. Procuranti B, Connon SJ. Unexpected catalysis: aprotic pyridinium ions as active and recyclable Bronsted acid catalysts in protic media. *Org Lett.* 2008; 10:4935–4938. [PubMed: 18837552]
28. Cacciapaglia R, Stefano SD, Mandolini L. Metathesis reaction of formaldehyde acetals: an easy entry into the dynamic covalent chemistry of cyclophane formation. *J Am Chem Soc.* 2005; 127:13666–13671. [PubMed: 16190732]
29. Mohr GJ, Spichiger-Keller UE. Novel fluorescent sensor membranes for alcohols based on *p*-*N,N*-dioctylamino-4'-trifluoroacetylstilbene. *Anal Chim Acta.* 1997; 351:189–196.
30. Matsui M, Yamada K, Funabiki K. Hemiacetal and hemiaminal formation at fluoroacyl moiety. *Tetrahedron.* 2005; 61:4671–4677.
31. Sasaki S, Kotegawa Y, Tamiaki H. Trifluoroacetyl-chlorin as a new chemosensor for alcohol/amine detection. *Tetrahedron Lett.* 2006; 47:4849–4852.
32. Joyce LA, Shabbir SH, Anslyn EV. The uses of supramolecular chemistry in synthetic methodology development: examples of anion and neutral molecular recognition. *Chem Soc Rev.* 2010; 39:3621–3632. [PubMed: 20714470]
33. Dounay AB, Humphreys PG, Overman LE, Wroblewski AD. Total synthesis of the strychnos alkaloid (+)-minfiensine: tandem enantioselective intramolecular Heck-iminium ion cyclization. *J Am Chem Soc.* 2008; 130:5368–5377. [PubMed: 18303837]
34. Jones SB, Simmons B, Mastracchio A, MacMillan DWC. Collective synthesis of natural products by means of organocascade catalysis. *Nature.* 2011; 475:183–188. [PubMed: 21753848]
35. Xu H, Zuend SJ, Woll MG, Tao Y, Jacobsen EN. Asymmetric cooperative catalysis of strong Bronsted acid-promoted reactions using chiral ureas. *Science.* 2010; 327:986–990. [PubMed: 20167783]
36. Li G, Fronczek FR, Antilla JC. Catalytic asymmetric addition of alcohols to imines: enantioselective preparation of chiral *N,O*-aminals. *J Am Chem Soc.* 2008; 130:12216–12217. [PubMed: 18722443]
37. Star A, Goldberg I, Fuchs B. Dioxadiazadecalin/salen tautomeric macrocycles and complexes: prototypal dynamic combinatorial virtual libraries. *Angew Chem Int Ed.* 2000; 39:2685–2689.

38. Terada M, Machioka K, Sorimachi K. Activation of hemiaminal ethers by chiral Brønsted acids for facile access to enantioselective two-carbon homologation using enecarbamates. *Angew Chem Int Ed.* 2009; 48:2553–2556.
39. You L, Long SR, Lynch VM, Anslyn EV. Dynamic multi-component hemiaminal assembly. *Chem Eur J.* 2011; 17:11017–11023. [PubMed: 21919095]
40. Leonard NJ, Paukstelis JV. Direct synthesis of ternary iminium salts by combination of aldehydes or ketones with secondary amine salts. *J Org Chem.* 1963; 28:3021–3024.
41. Kütt A, et al. A comprehensive self-consistent spectrophotometric acidity scale of neutral Brønsted acids in acetonitrile. *J Org Chem.* 2006; 71:2829–2838. [PubMed: 16555839]
42. Kaljurand I, et al. Extension of the self-consistent spectrophotometric basicity scale in acetonitrile to a full span of 28 p*K_a* units: unification of different basicity scales. *J Org Chem.* 2005; 70:1019–1028. [PubMed: 15675863]
43. Zhang L, Clark RJ, Zhu L. A heteroditopic fluoroionophoric platform for constructing fluorescent probes with large dynamic ranges for zinc ions. *Chem Eur J.* 2008; 14:2894–2903. [PubMed: 18232042]
44. Gruenwedel DW. Multidentate coordination compounds. Chelating properties of aliphatic amines containing -pyridyl residues and other aromatic ring systems as donor groups. *Inorg Chem.* 1968; 7:495–501.
45. Reetz MT. Combinatorial and Evolution-Based Methods in the Creation of Enantioselective Catalysts. *Angew Chem Int Ed.* 2001; 40:284–310.
46. Castagnetto JM, Xu X, Berova ND, Canary JW. Absolute configurational assignment of self-organizing asymmetric tripodal ligand-metal complexes. *Chirality.* 1997; 9:616–622. [PubMed: 9329182]
47. Zahn S, Canary JW. Electron-induced inversion of helical chirality in copper complexes of *N,N*-dialkylmethionines. *Science.* 2000; 288:1404–1407. [PubMed: 10827947]
48. Berova N, Di Bari L, Pescitelli G. Application of electronic circular dichroism in configurational and conformational analysis of organic compounds. *Chem Soc Rev.* 2007; 36:914–931. [PubMed: 17534478]
49. Ghosn MW, Wolf C. Chiral amplification with a stereodynamic triaryl probe: assignment of the absolute configuration and enantiomeric excess of amino alcohols. *J Am Chem Soc.* 2009; 131:16360–16361. [PubMed: 19902975]
50. Li X, Tanasova M, Vasileiou C, Borhan B. Fluorinated porphyrin tweezer: a powerful reporter of absolute configuration for erythro and threo diols, amino alcohols, and diamines. *J Am Chem Soc.* 2008; 130:1885–1893. [PubMed: 18211067]
51. Li X, Borhan B. Prompt determination of absolute configuration for epoxy alcohols via exciton chirality protocol. *J Am Chem Soc.* 2008; 130:16126–16127. [PubMed: 18998673]
52. Lintuluoto JM, Borovkov VV, Inoue Y. Direct determination of absolute configuration of monoalcohols by bis(magnesium porphyrin). *J Am Chem Soc.* 2002; 124:13676–13677. [PubMed: 12431088]

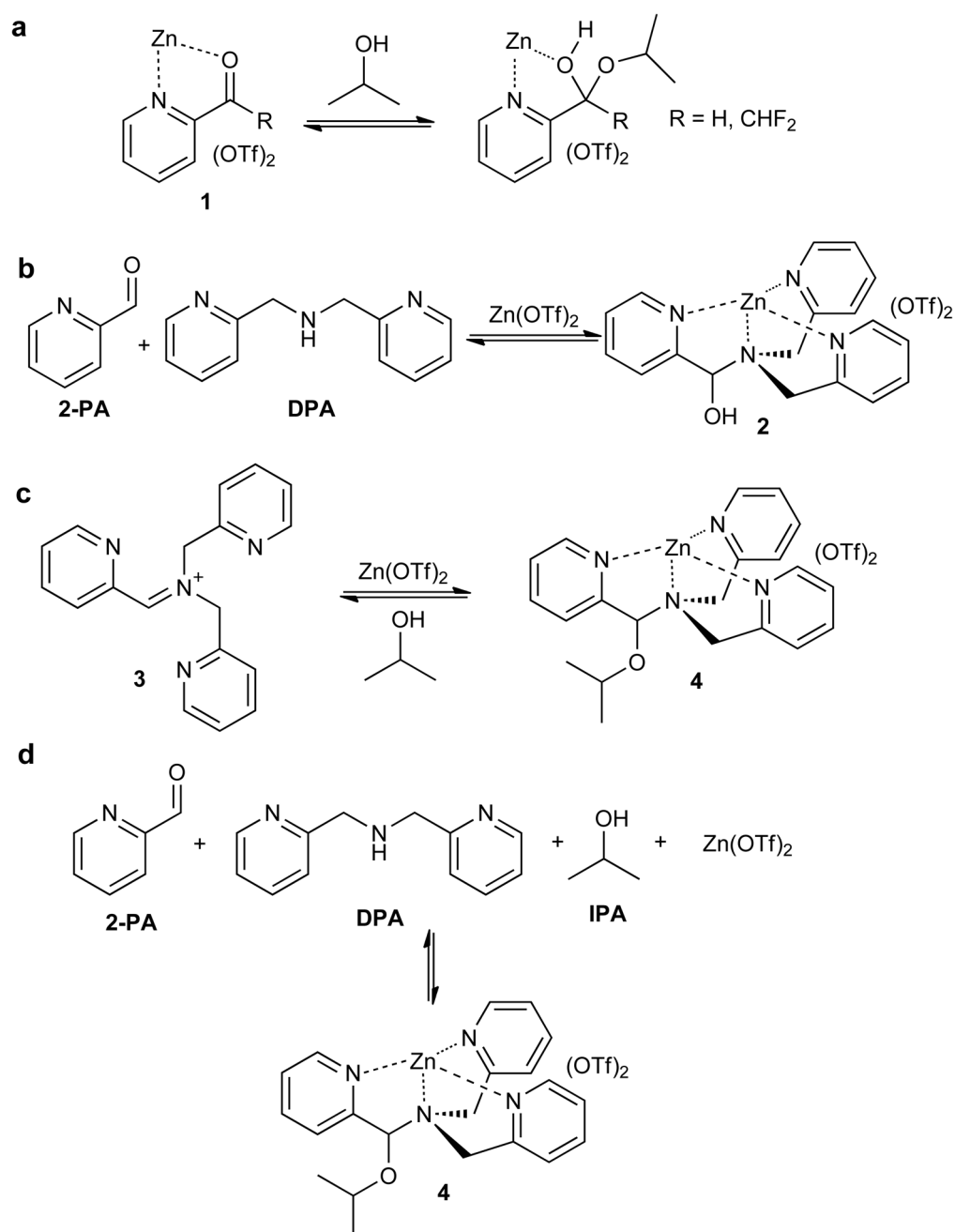


Figure 1. Proposed solution to the challenge of the binding of secondary alcohols
a, Lewis acid activation of carbonyls *via* chelation control, and the reversible binding of secondary alcohols to give hemiacetals. **b**, Zinc-templated three-component dynamic assembly to create a hemiaminal **2**. **c**, Proposed tris(pyridine) based iminium **3** for alcohol binding and metal complex formation. **d**, Our four-component reversible covalent assembly for secondary alcohol binding, likely through iminium ion **3** as an intermediate. OTf = trifluoromethanesulfonate (triflate).

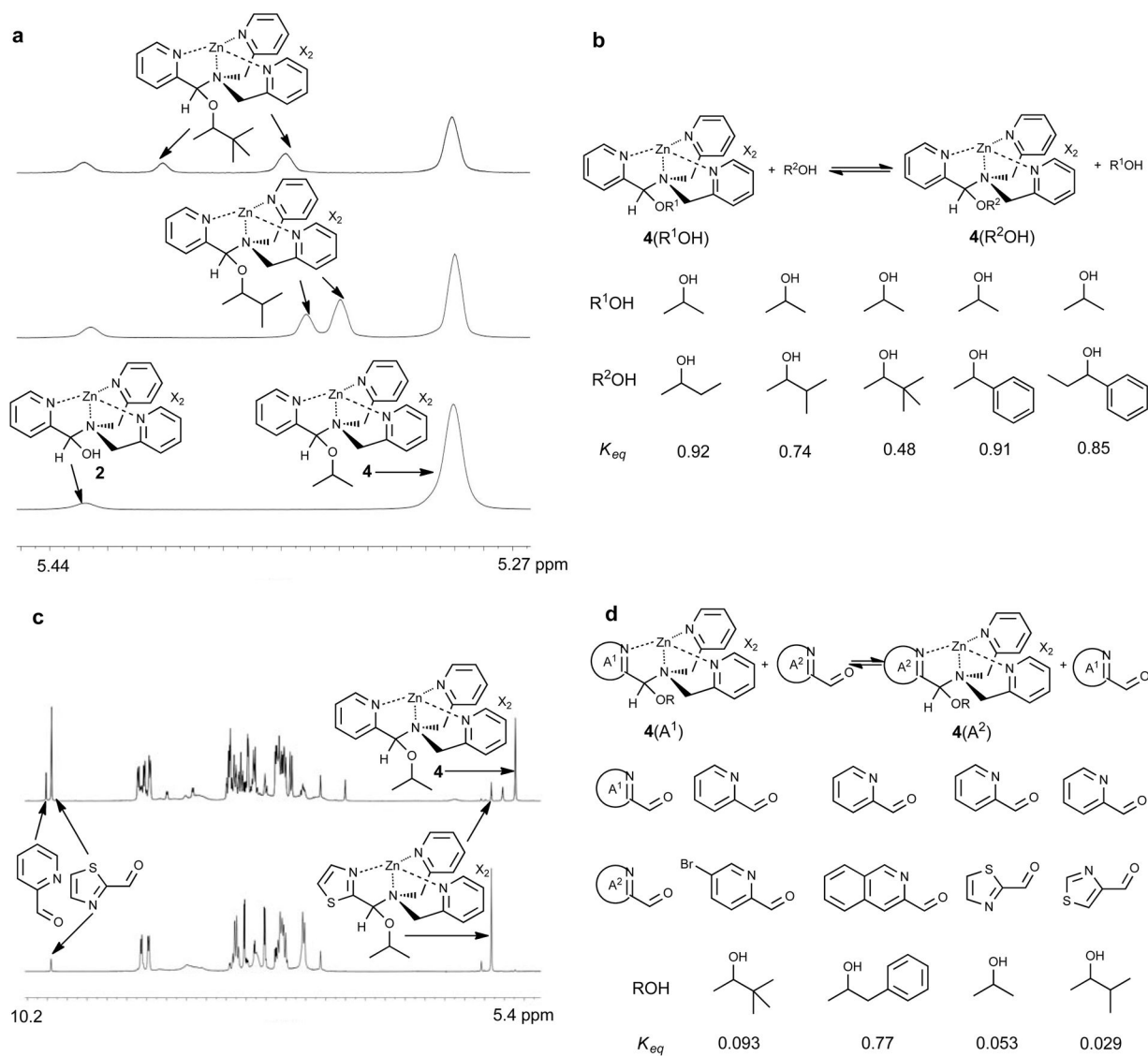


Figure 2. Component exchange within the multi-component assembly

a, Exchange of IPA derived assembly **4** (bottom panel) with 3-methyl-2-butanol (middle panel) and with 3,3-dimethyl-2-butanol (top panel). Only the methine portion of the 1H NMR spectra is shown. **b**, The structures of the alcohols and their respective equilibrium constants for exchange. $K_{eq} = [4(R^2OH)][R^1OH]/\{[4(R^1OH)][R^2OH]\}$. **c**, Exchange of thiazole-2-carboxaldehyde derived assembly (bottom panel) with **2-PA** (top panel). Resonance from thiazole-2-carboxaldehyde at 10 ppm increased. **d**, The structures of the aldehydes and their respective equilibrium constants for exchange. $K_{eq} = [4(A^2)][A^1]/\{[4(A^1)][A^2]\}$. X is the counterion for zinc (chloride or triflate).

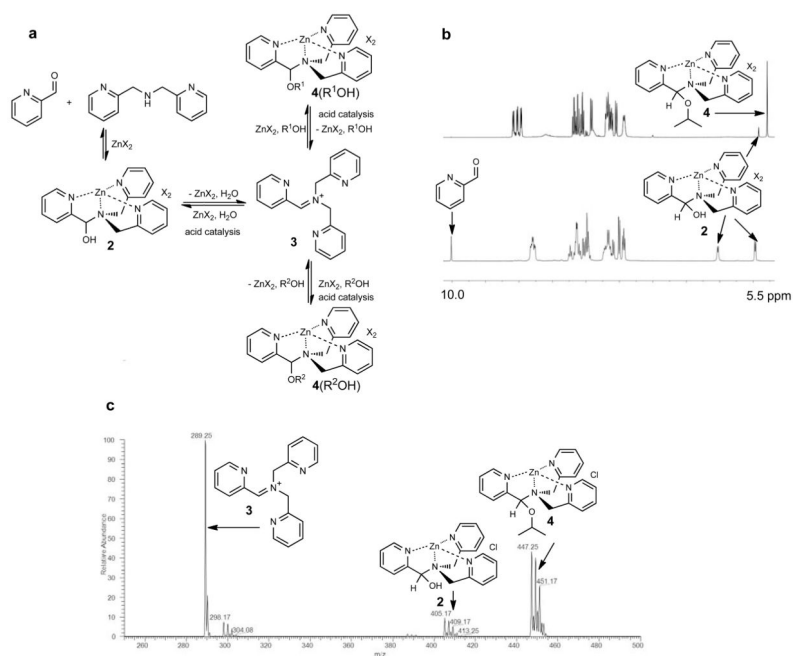


Figure 3. Experimental evidence, and proposed mechanism for the multi-component assembly a. Proposed mechanism for formation of **4** that also explains the reversible exchange of alcohols and aldehydes. **b.** A three-component assembly of **2-PA**, **DPA**, and **Zn(OTf)₂** to form **2** with molecular sieves (bottom panel) upon addition of **IPA** and **CEM-HCl** led to the same complex **4** (top panel) as a four-component reaction. The arrows indicate that these peaks belong to the structures shown. **c.** ESI mass spectrum of **IPA** derived assembly. Peaks of **2**, **3**, and **4** were all observed with chloride as counter anion for **2** and **4**.

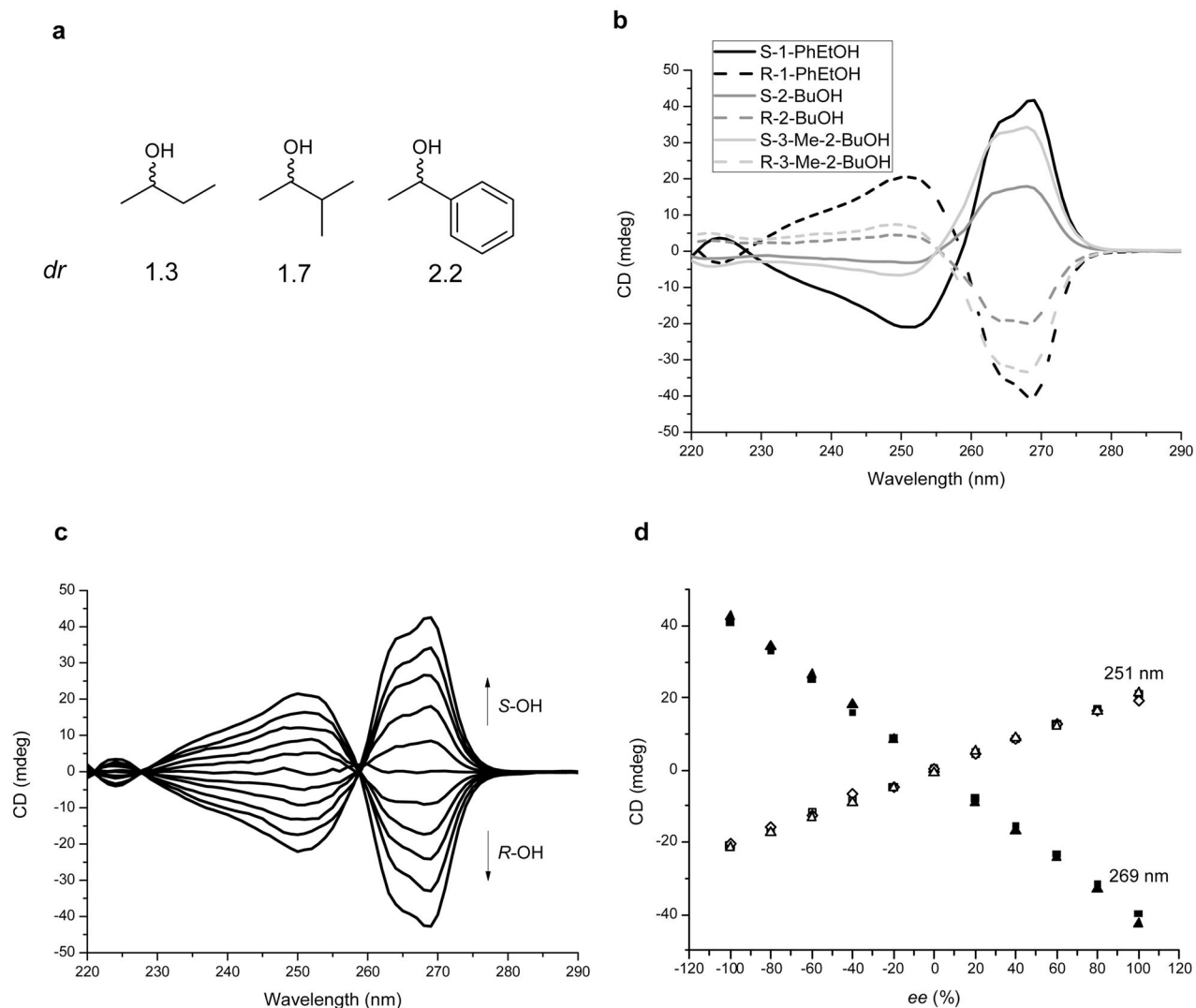


Figure 4. Exploration of four-component assembly for chirality sensing and *ee* determination
a, *dr* values for assemblies with chiral mono-ols (*R* or *S*) obtained from ^1H NMR. **b**, CD spectra of assembly derived from three alcohols (0.175 mM **2-PA**, 0.525 mM mono-ol). **c**, CD spectra of 1-phenylethanol derived assembly with different *ee* of alcohol (from top to bottom: *ee* -100, -80, -60, -40, -20, 0, 20, 40, 60, 80, 100 %, 0.175 mM **2-PA**, 0.525 mM 1-phenylethanol). **d**, Linear *ee* calibration line at 251 nm and 269 nm (For all experiments, 35 mM of **2-PA** was used for assembly reaction).